

Fast recovery of the stripe magnetic order by Mn/Fe substitution in F-doped LaFeAsO superconductors

M. Moroni,^{1,*} P. Carretta,¹ G. Allodi,² R. De Renzi,² M. N. Gastiasoro,³ B. M. Andersen,³ P. Materne,⁴ H.-H. Klauss,⁴ Y. Kobayashi,⁵ M. Sato,⁵ and S. Sanna^{1,6}

¹*Department of Physics, University of Pavia-CNISM, I-27100 Pavia, Italy*

²*Dipartimento di Fisica e Scienze della Terra, Università di Parma, I-43124 Parma, Italy*

³*Niels Bohr Institute, University of Copenhagen, Juliane Maries Vej 30, 2100 Copenhagen, Denmark*

⁴*Institute of Solid State Physics, TU Dresden, D-01069 Dresden, Germany*

⁵*Department of Physics, Division of Material Sciences, Nagoya University, Furo-cho, Chikusa-ku, Nagoya 464-8602, Japan*

⁶*Department of Physics and Astronomy, University of Bologna, 40127 Bologna, Italy*

(Received 2 December 2016; published 9 May 2017)

⁷⁵As nuclear magnetic (NMR) and quadrupolar (NQR) resonance were used, together with Mössbauer spectroscopy, to investigate the magnetic state induced by Mn for Fe substitutions in F-doped LaFe_{1-x}Mn_xAsO superconductors. The results show that 0.5% of Mn doping is enough to suppress the superconducting transition temperature T_c from 27 K to zero and to recover the magnetic structure observed in the parent undoped LaFeAsO. Also the tetragonal to orthorhombic transition of the parent compound is recovered by introducing Mn, as evidenced by a sharp drop of the NQR frequency. The NQR spectra also show that a charge localization process is at play in the system. Theoretical calculations using a realistic five-band model show that correlation-enhanced RKKY exchange interactions between nearby Mn ions stabilize the observed stripe magnetic order. These results give compelling evidence that F-doped LaFeAsO is a strongly correlated electron system at the verge of an electronic instability.

DOI: [10.1103/PhysRevB.95.180501](https://doi.org/10.1103/PhysRevB.95.180501)

The interplay between impurity induced disorder and electronic correlations often gives rise to complex phase diagrams in condensed matter [1,2]. The electronic correlations drive a system towards a quantum phase transition, as it is typically found in the fullerenes [3] and in heavy-fermion compounds [4,5], with an enhancement of the local susceptibility and, hence, a small perturbation, as the one associated with a tiny amount of impurities, can significantly affect the electronic ground state [6–9]. In the cuprates and in the electron-doped iron-based superconductors (IBS), the strength of the electronic correlations can be tuned either by charge doping or by applying an external or a chemical pressure [10–14]. In particular, upon increasing the charge doping, the strength of the electronic correlations tend to decrease [15–22] and a metallic Fermi liquid (FL) ground state is usually restored [23–27]. However, significant electronic correlations may still be present even close to the charge doping levels yielding the maximum superconducting transition temperature T_c and a convenient method to test their magnitude is to perturb the system with impurities.

The introduction of Mn impurities at the Fe sites was reported to strongly suppress T_c in several IBS, both of the BaFe₂As₂ [28–30] and of the LnFeAsO (Ln1111, Ln=lanthanides) [31] families. Within the Ln1111 family the effect of impurities is particularly significant in La1111 [27,32]. In fact, while in most the IBS compounds the T_c suppression rate (dT_c/dx) is well below 10 K/% Mn, in LaFeAsO_{0.89}F_{0.11} just 0.2%–0.3% of Mn impurities suppress superconductivity from the optimal $T_c \simeq 27$ K ($dT_c/dx \sim 110$ K/% Mn) and then, at higher Mn doping levels,

a magnetic order develops [see Fig. 1(b)] [32–34]. The understanding of why such a dramatic effect is present, what type of magnetic order is developing and how to describe these materials at the microscopic level are presently subject of debate [35–37]. Here we show, by means of zero-field (ZF) NMR, nuclear quadrupole resonance (NQR), and Mössbauer spectroscopy that the introduction of 0.5% of Mn in LaFeAsO_{0.89}F_{0.11} induces the recovery of the magnetic order and of the tetragonal to orthorhombic (T-O) structural transitions observed in LaFeAsO, the parent compound of La1111 superconductors. Moreover, the decrease of the charge transfer integral and the enhanced electron correlations lead to the electron localization and to a local charge distribution similar to that found in LaFeAsO. We also present theoretical calculations showing that correlation-enhanced RKKY exchange couplings between neighboring Mn ions stabilize the magnetic order characterized by $Q_1 = (\pi, 0)$ and $Q_2 = (0, \pi)$ domains.

The LaFe_{1-x}Mn_xAsO_{0.89}F_{0.11} polycrystalline samples under investigation are the same ones studied in Ref. [32]. Further details on the sample preparation and characterization can be found in Ref. [38].

⁷⁵As zero-field (ZF) NMR spectra were obtained by recording the echo amplitude as a function of the irradiating frequency in the 6–26 MHz range for $T = 8$ K [see Fig. 1(a)]. Both the spectra of the LaFeAsO parent compound and of the $x = 0.75\%$ sample are characterized by two peaks, which in the latter compound are rigidly shifted to lower frequencies and broadened. The peaks are associated with the $m_I = 1/2 \rightarrow m_I = -1/2$ and $m_I = -1/2 \rightarrow m_I = -3/2$ transitions, with m_I the component of the nuclear spin I along the quantization axis, which in the case of a stripe magnetic order [magnetic wave vector $Q = (\pi, 0)$ or $(0, \pi)$], as it is the case for

*matteo.moroni01@universitadipavia.it

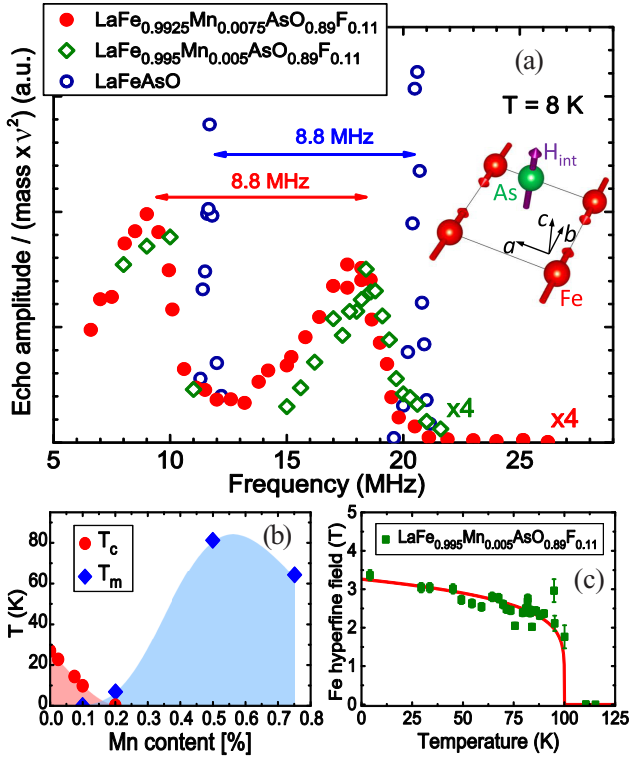


FIG. 1. (a) Comparison of the ^{75}As zero-field NMR spectra between the LaFeAsO parent compound and $\text{LaFe}_{1-x}\text{Mn}_x\text{AsO}_{0.89}\text{F}_{0.11}$ for $x = 0.5\%$ (green) and 0.75% (red). For the sake of comparison, the intensity of the spectra for the Mn-substituted compounds is multiplied by 4. (Inset) Sketch of the magnetic unit cell for the stripe order (the red arrows represent the Fe magnetic moments directions while the magenta arrow corresponds to the orientation of the internal field at the As site). (b) Electronic phase diagram of $\text{LaFe}_{1-x}\text{Mn}_x\text{AsO}_{0.89}\text{F}_{0.11}$. T_c and T_m were determined from magnetization (SQUID) and zero-field μSR measurements, respectively (see Ref. [32]). (c) Temperature dependence of the hyperfine magnetic field, B_h , for $x = 0.5\%$ as derived from Mössbauer spectra. The red solid line tracking the order parameter is a phenomenological fit of B_h with $B_h = 3.3(1 - (T/T_m))^\beta$ where $T_m = 100\text{ K}$ and $\beta = 0.17$.

LaFeAsO , is along the c axis. The frequency shift between the two peaks is given by the nuclear quadrupole frequency determined by the local charge distribution, which at 8 K is $\nu_Q = 8.8\text{ MHz}$ both for LaFeAsO and for the $x = 0.75\%$ sample.

The position of the low-frequency peak (ν_c), associated with the $1/2 \rightarrow -1/2$ transition, is determined by the magnitude of the hyperfine field at ^{75}As , and one can write that $\nu_c = (\gamma/2\pi)|\mathcal{A}\langle\vec{S}\rangle|$, with γ the ^{75}As gyromagnetic ratio, \mathcal{A} the hyperfine coupling tensor, and $\langle\vec{S}\rangle$ the average electron spin, corresponding to the magnetic phase order parameter. Accordingly, the low-frequency shift of the two peaks in the sample with $x = 0.75\%$ would indicate a reduction of the order parameter to about 80% of the value found for LaFeAsO . The sample with $x = 0.5\%$ displays a very similar behavior with a slight increase in the low-temperature order parameter, following its slightly higher magnetic transition temperature (T_m) [32]. From the magnetic point of view, the two samples

$x = 0.5\%$ and 0.75% are almost equivalent, as already shown from previous muon spin relaxation experiments [32].

In order to further study the magnetic order parameter, we measured the temperature dependence of Mössbauer spectra for the $x = 0.5\%$ sample. Figure 1(c) shows that in the low-temperature limit the internal field at the Fe site is of about 3.5 T , i.e., the magnitude of the order parameter is reduced to about 70% of the value found in pure LaFeAsO [39–41], in reasonable agreement with what we derived above from ZF-NMR.

Now, one has first to consider if magnetic orders different from the stripe one could give rise to a similar ZF-NMR spectrum, taking into account the reduction in the Fe moment to about 80% of the value found in LaFeAsO . The other low-energy magnetic orders that could develop in this compound are the Néel [$Q = (\pi, \pi)$] and the orthomagnetic type, with a $\pi/2$ rotation of the adjacent spins [25]. Calculations of the hyperfine magnetic field [42,43] at the As site (see Ref. [38]) show that both these magnetic orders would give rise to ZF-NMR lines significantly shifted from the ones reported in Fig. 1(a), thus confirming that the order is stripe-type. On the other hand, one could argue that the stripe order could coexist with other types of order developing close to Mn impurities and that we are actually detecting the signal from a fraction of ^{75}As nuclei only. Thus we have performed a quantitative estimate of the amount of nuclei contributing to the $x = 0.75\%$ sample ZF-NMR spectrum in Fig. 1(a) by comparing its integrated intensity with that of the LaFeAsO sample, where 100% of the sample is in the stripe collinear phase. We found that $95 \pm 5\%$ of the $x = 0.75\%$ sample is in the stripe order.

In order to further check if there is a small ($\leq 5\%$) fraction of ^{75}As nuclei that we are missing, we performed ^{75}As NMR measurements in a 8 T magnetic field. In Fig. 2, the powder NMR spectrum displays a large fraction of nuclei with a spectrum broadened [44] by the internal field developing in the stripe phase (cyan diamonds) as well as a small fraction

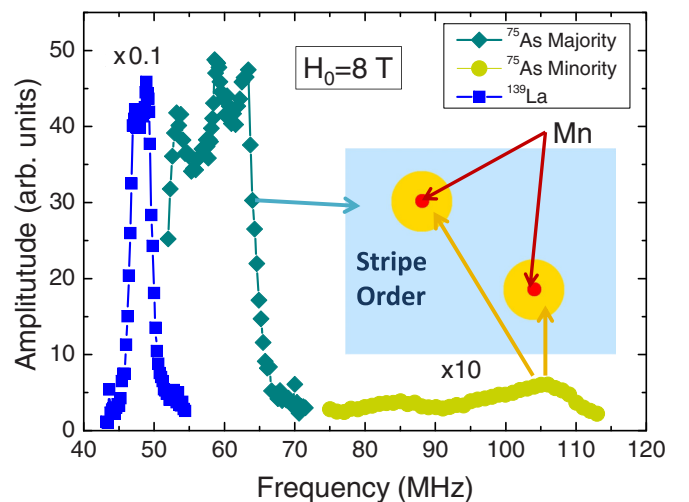


FIG. 2. $\text{LaFe}_{1-x}\text{Mn}_x\text{AsO}_{0.89}\text{F}_{0.11}$ ($x = 0.5\%$) ^{75}As and ^{139}La NMR spectra in the $40\text{--}115\text{ MHz}$ frequency range, measured at 10 K , for an applied magnetic field $\mu_0 H = 8\text{ T}$. (Inset) Pictorial representation of the Fe layer for a few parts per thousand of Mn substitution in $\text{LaFeAsO}_{0.89}\text{F}_{0.11}$.

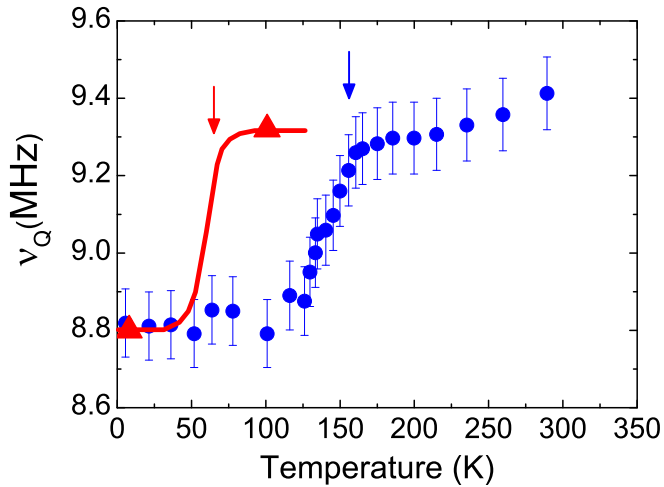


FIG. 3. Quadrupolar frequency ν_Q as a function of temperature for the LaFeAsO (blue circles, data from Ref. [45]) and LaFe $_{1-x}$ Mn $_x$ AsO $_{0.89}$ F $_{0.11}$ with $x = 0.75\%$ (red triangles). For the latter, the point above T_m is taken as the frequency of the low-frequency peak of Fig. 4(a) (see text). The vertical arrows indicate the magnetic transitions, while the red solid line is a guide to the eye.

of about $3\% \pm 1\%$ of ^{75}As nuclei with a significant NMR shift towards higher frequencies (yellow circles). These latter nuclei are likely the ones close to Mn impurities where a large hyperfine field is expected. For $x = 0.5\%$, there are 2% of As nuclei, which are nearest neighbors of a Mn impurities, a value very similar to the one we found. Hence the introduction of Mn suppresses superconductivity and leads to the recovery of the stripe magnetic order found in the parent LaFeAsO compound. Any incommensurate magnetic order, if present, should have a magnetic wave vector very close to the stripe one (see Ref. [38]). This aspect could be clarified by future neutron diffraction experiments.

The nuclear quadrupole frequency (Fig. 3) shows a jump on passing from just above T_m (^{75}As NQR) to below T_m (^{75}As ZF-NMR), which is very similar to the one detected [45] in LaFeAsO. This abrupt change in ν_Q is associated with the T-O distortion. Therefore the observation of a similar change in ν_Q for the $x = 0.5\%$ compound indicates that when the stripe magnetic order is recovered by Mn doping, also the T-O structural transition is recovered, confirming that this transition is closely related to the onset of large stripe magnetic correlations. We further remark that the T-O transition causes also a change in the electric field gradient probed by Fe nuclei, as detected by Mössbauer spectroscopy (see Ref. [38]).

Another relevant aspect can be grasped by looking at the ^{75}As NQR spectra, which can give detailed information about the electronic environment surrounding the As nuclei [46–48]. The spectra in Fig. 4, measured at $T = 77\text{ K}$ for $x \leq 0.2\%$ and at $T = 100\text{ K}$ (above T_m) for $x > 0.2$ show a clear shift of the NQR spectrum towards lower frequency with increasing Mn content [see Fig. 4(b)] and a rapid change in the intensity of the low-frequency peak for $x > 0.2\%$. It is worth to note that for $x > 0.2\%$ the frequency of the dominant low-frequency peak perfectly matches that of the paramagnetic phase of LaFeAsO [see Figs. 3 and 4(b)], indicating a similar

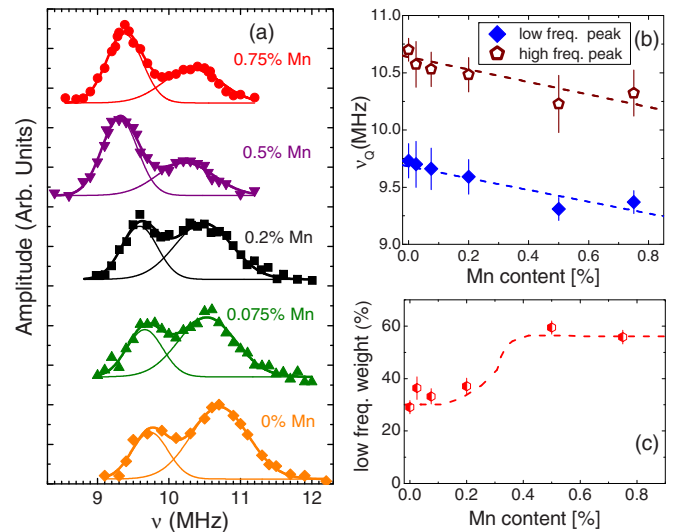


FIG. 4. (a) ^{75}As NQR spectra of LaFe $_{1-x}$ Mn $_x$ AsO $_{0.89}$ F $_{0.11}$ for different Mn contents, measured at $T = 77\text{ K}$ for $x \leq 0.2\%$ and $T = 100\text{ K}$ (above T_m) for $x > 0.2\%$. The solid lines are fits to a sum of two Gaussian functions. (b) Frequency of the low- (blue diamonds) and high-energy (red pentagons) peaks as a function of Mn content. The dashed lines are a guide to the eye. (c) Weight of the low-frequency peak as a function of Mn content, the dashed line is a guide to the eye.

electronic ground state. According to Lang *et al.* [47], the low- and high-frequency NQR peaks should be associated with nanoscopically segregated regions with different electron doping levels. In particular, the low-frequency peak should be associated with a lower electronic concentration of weakly itinerant electrons. Hence the increase in the magnitude of the low-frequency peak above $x = 0.2\%$ indicates a tendency towards electron localization. This finding is also corroborated by the rapid increase of the electric resistivity as a function of Mn content previously observed [31,49] across the metal-insulator crossover taking place around $x = 0.2\%$. A similar rise in resistivity was also observed [16] in LaFeAsO $_{1-x}$ F $_x$ with decreasing F content. One would expect that since LaFeAsO $_{1-x}$ F $_x$ is characterized by Fermi pockets, a scattering center such as Mn would induce in any way charge localization. However, this can occur only if the response function of the bare system is strongly enhanced, as it is the case for La1111 but not for Sm1111. We add here that the increase of the resistivity and the slight increase of the lattice constant c follow the suppression of the superconductivity (see Fig. 12 of Ref. [31] for details). In fact, the c axis value appears to correlate with the T_c value, irrespective of the microscopic mechanism of suppression.

In order to further clarify the origin of the dramatic effect of Mn doping in LaFeAsO $_{0.89}$ F $_{0.11}$, we carried out real space theoretical calculations using a realistic five-band Hamiltonian [27,50] (see Ref. [38]). In Ref. [27], it was demonstrated that in this framework the enhanced spin correlations developing around Mn severely speed up the reduction of T_c driven by the magnetic disorder, and may quench the entire superconducting phase already at Mn concentrations below 1% . The Mn moments, while substituting random

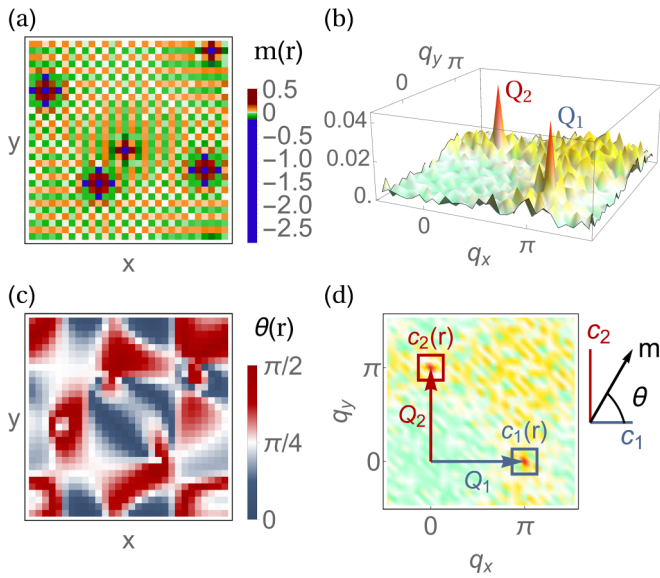


FIG. 5. (a) Induced magnetic order $m(r)$ for 0.55% Mn moments and (b) its Fourier transform $|m(q)|$. (c) Local phase map $\theta(r) = \arctan(|c_1(r)|/|c_2(r)|)$ showing the ordering vectors on the lattice: $\theta = 0$ and $\pi/2$ for single- Q Q_1 (blue) and Q_2 (red) domains, respectively, and $\theta = \pi/4$ for double- Q regions (white). The coefficient associated with Q_1 (Q_2), $c_1(r) = \sum_n c_n \exp[i(q_n - Q_1)r]$, is calculated by a filtered Fourier transform with the $\{q_n\}$ wave vectors contained inside the blue and red squares shown in panel (d). The inset illustrates the definition of the local phase $\theta(r)$.

Fe positions, orient their moments favorably to generate a long-range ordered SDW phase, which minimizes the total free energy of systems at the brink of a SDW instability [51,52].

In Fig. 5(a), we show the total magnetization for a collection of 0.55% Mn ions randomly placed in the square Fe lattice. This concentration of Mn is able to fully suppress T_c and spin polarize all Fe sites (which were all nonmagnetic without Mn impurity ions). The Mn-induced magnetic order existing in the interimpurity regions is long-ranged as reproduced by the sharp peaks in Fig. 5(b), which are absent in the Mn-free compound. A small fraction of the sites, roughly corresponding to the Mn sites and to their nearest neighbors (amounting to $\sim 5\%$ of the lattice) exhibits a significantly larger moment, in overall agreement with the above discussion of the ^{75}As NMR data (see Fig. 2).

The magnetic order generated by Mn doping is efficiently stabilized due to correlation-enhanced RKKY exchange couplings between neighboring Mn ions. The structure of the induced order is thus dictated by the susceptibility of the bulk itinerant system, which, in the present case, is peaked at $Q_1 = (\pi, 0)$ and $Q_2 = (0, \pi)$ regions. In Fig. 5(c), we provide a real-space map of the dominant momentum structure by

utilizing a filtered Fourier transform illustrated in Fig. 5(d) and the associated caption. As seen, the system breaks up into regions of single- Q domains, i.e., either Q_1 - or Q_2 -dominated regions, and does not exhibit substantial volume fraction of a double- Q order [37]. This is consistent with the presence of a (reduced) orthorhombic transition associated with the Mn-induced magnetic order, as found by ^{75}As NQR (see Fig. 3). All these theoretical results match with the experimental outcomes.

Overall, the above scenario is a clear indication that in $\text{LaFeAsO}_{0.89}\text{F}_{0.11}$, superconductivity emerges from a strongly correlated electron system close to a metal-insulator transition. The electron correlations are so strong that, owing to the enhanced spin susceptibility at $Q = (\pi, 0)$, the effect of a tiny amount of impurities extends over many lattice sites, giving rise to a sizable RKKY coupling among them, able to abruptly destroy superconductivity and to restore the stripe magnetic order. The onset of the magnetic order is intimately related with the charge localization [31] and hence to the T_c suppression. This situation is reminiscent of the phenomenology observed in heavy fermion (HF) compounds [53,54] where the FL phase vanishes and a magnetic order arises in correspondence of a QCP when the RKKY interaction overcomes the Kondo coupling. For example, in CeCoIn_5 , a HF compound, it was shown that a tiny amount of Cd doping restores the long-range antiferromagnetic (AF) order [4,5,55] and suppresses the superconducting dome developing around the quantum critical point separating the FL from the AF phase. In $\text{LaFe}_{1-x}\text{Mn}_x\text{AsO}_{0.89}\text{F}_{0.11}$ the Kondo coupling would involve itinerant and more localized $3d$ electrons [19,56,57] playing a role analogous to the f electrons in the HF. When these latter electrons finally localize, the RKKY coupling among Mn impurities leads to the recovery of magnetism and the suppression of the metallic superconducting state.

The abrupt suppression of the superconducting phase and the recovery of the magnetic order and of the structural T-O transition give compelling evidence that the optimally F-doped LaFeAsO is at the verge of an electronic instability, close to a QCP [32]. Previous experimental results have shown that this system can be driven away from the QCP via the total substitution of La with Nd or by the partial substitution with Y [33,34], which shrink the structure and cause a reduction of the electronic correlations [27]. Hence the Ln1111 compound can be considered as a formidable example of how the electronic properties of strongly correlated systems can be significantly affected by fine-tuning the correlation strength with impurities and chemical pressure.

B. Büchner is thanked for useful discussions. This work was supported by MIUR-PRIN2012 Project No. 2012X3YFZ2. M.N.G. and B.M.A acknowledge support from Lundbeckfond fellowship (Grant No. A9318).

- [1] E. Miranda and V. Dobrosavljevic, *Rep. Prog. Phys.* **68**, 2337 (2005).
 [2] P. A. Lee and T. V. Ramakrishnan, *Rev. Mod. Phys.* **57**, 287 (1985).

- [3] Y. Nomura, S. Sakai, M. Capone, and R. Arita, *Sci. Adv.* **1**, e1500568 (2015).
 [4] S. Seo, Xin Lu, J-X. Zhu, R. R. Urbano, N. Curro, E. D. Bauer, V. A. Sidorov, L. D. Pham, Tuson Park,

- Z. Fisk, and J. D. Thompson, *Nat. Phys.* **10**, 120 (2014).
- [5] A. Benali, Z. J. Bai, N. J. Curro, and R. T. Scalettar, *Phys. Rev. B* **94**, 085132 (2016).
- [6] H. Alloul, J. Bobroff, M. Gabay, and P. J. Hirschfeld, *Rev. Mod. Phys.* **81**, 45 (2009).
- [7] M. Sato, Y. Kobayashi, S. Satomi, T. Kawamata, and M. Itoh, *J. Phys.: Conf. Ser.* **400**, 022104 (2012).
- [8] S. Sanna, P. Carretta, R. De Renzi, G. Prando, P. Bonfà, M. Mazzani, G. Lamura, T. Shiroka, Y. Kobayashi, and M. Sato, *Phys. Rev. B* **87**, 134518 (2013).
- [9] G. Prando, Th. Hartmann, W. Schottenhamel, Z. Guguchia, S. Sanna, F. Ahn, I. Nekrasov, C. G. F. Blum, A. U. B. Wolter, S. Wurmehl, R. Khasanov, I. Eremin, and B. Büchner, *Phys. Rev. Lett.* **114**, 247004 (2015).
- [10] H. Luetkens, H.-H. Klauss, R. Khasanov, A. Amato, R. Klingeler, I. Hellmann, N. Leps, A. Kondrat, C. Hess, A. Kohler, G. Behr, J. Werner, and B. Büchner, *Nat. Mater.* **8**, 305 (2009).
- [11] S. Sanna, R. De Renzi, G. Lamura, C. Ferdeghini, A. Palenzona, M. Putti, M. Tropeano, and T. Shiroka, *Phys. Rev. B* **80**, 052503 (2009).
- [12] T. Shiroka, G. Lamura, S. Sanna, G. Prando, R. De Renzi, M. Tropeano, M. R. Cimberle, A. Martinelli, C. Bernini, A. Palenzona, R. Fittipaldi, A. Vecchione, P. Carretta, A. S. Siri, C. Ferdeghini, and M. Putti, *Phys. Rev. B* **84**, 195123 (2011).
- [13] G. Prando, O. Vakaliuk, S. Sanna, G. Lamura, T. Shiroka, P. Bonfà, P. Carretta, R. De Renzi, H.-H. Klauss, C. G. F. Blum, S. Wurmehl, C. Hess, and B. Büchner, *Phys. Rev. B* **87**, 174519 (2013).
- [14] R. Khasanov, S. Sanna, G. Prando, Z. Shermadini, M. Bendele, A. Amato, P. Carretta, R. De Renzi, J. Karpinski, S. Katrych, H. Luetkens, and N. D. Zhigadlo, *Phys. Rev. B* **84**, 100501 (2011).
- [15] M. Capone, M. Fabrizio, C. Castellani, and E. Tosatti, *Science* **296**, 2364 (2002).
- [16] C. Hess, A. Kondrat, A. Narduzzo, J. E. Hamann-Borrero, R. Klingeler, J. Werner, G. Behr, and B. Büchner, *Europhys. Lett.* **87**, 17005 (2009).
- [17] M. M. Qazilbash, J. J. Hamlin, R. E. Baumbach, L. Zhang, D. J. Singh, M. B. Maple, and D. N. Basov, *Nat. Phys.* **5**, 647 (2009).
- [18] H. Ikeda, R. Arita, and J. Kunes, *Phys. Rev. B* **82**, 024508 (2010).
- [19] P. Dai, J. Hu, and E. Dagotto, *Nat. Phys.* **8**, 709 (2012).
- [20] R. Yu, Q. Si, P. Goswami, and E. Abrahams, *J. Phys.: Conf. Ser.* **449**, 012025 (2013).
- [21] L. de Medici, G. Giovannetti, and M. Capone, *Phys. Rev. Lett.* **112**, 177001 (2014).
- [22] H. Lee, Y.-Z. Zhang, H. O. Jeschke, and R. Valenti, *Phys. Rev. B* **81**, 220506 (2010).
- [23] I. I. Mazin, D. J. Singh, M. D. Johannes, and M. H. Du, *Phys. Rev. Lett.* **101**, 057003 (2008).
- [24] M. Tropeano, M. R. Cimberle, C. Ferdeghini, G. Lamura, A. Martinelli, A. Palenzona, I. Pallecchi, A. Sala, I. Sheikin, F. Bernardini, M. Monni, S. Massidda, and M. Putti, *Phys. Rev. B* **81**, 184504 (2010).
- [25] G. Giovannetti, C. Ortix, M. Marsman, M. Capone, J. van den Brink, and J. Lorenzana, *Nat. Commun.* **2**, 398 (2011).
- [26] L. Benfatto, E. Cappelluti, L. Ortenzi, and L. Boeri, *Phys. Rev. B* **83**, 224514 (2011).
- [27] M. N. Gastiasoro, F. Bernardini, and B. M. Andersen, *Phys. Rev. Lett.* **117**, 257002 (2016).
- [28] P. Cheng, B. Shen, J. Hu, and H.-H. Wen, *Phys. Rev. B* **81**, 174529 (2010).
- [29] J. Li, Y. F. Guo, S. B. Zhang, J. Yuan, Y. Tsujimoto, X. Wang, C. I. Sathish, Y. Sun, S. Yu, W. Yi, K. Yamaura, E. Takayama-Muromachiu, Y. Shirako, M. Akaogi, and H. Kontani, *Phys. Rev. B* **85**, 214509 (2012).
- [30] D. LeBoeuf, Y. Texier, M. Boselli, A. Forget, D. Colson, and J. Bobroff, *Phys. Rev. B* **89**, 035114 (2014).
- [31] M. Sato, Y. Kobayashi, S. C. Lee, H. Takahashi, E. Satomi, and Y. Miura, *J. Phys. Soc. Jpn.* **79**, 014710 (2010).
- [32] F. Hammerath, P. Bonfà, S. Sanna, G. Prando, R. De Renzi, Y. Kobayashi, M. Sato, and P. Carretta, *Phys. Rev. B* **89**, 134503 (2014).
- [33] F. Hammerath, M. Moroni, L. Bossoni, S. Sanna, R. Kappenberger, S. Wurmehl, A. U. B. Wolter, M. A. Afrassa, Y. Kobayashi, M. Sato, B. Büchner, and P. Carretta, *Phys. Rev. B* **92**, 020505(R) (2015).
- [34] M. Moroni, S. Sanna, G. Lamura, T. Shiroka, R. De Renzi, R. Kappenberger, M. A. Afrassa, S. Wurmehl, A. U. B. Wolter, B. Büchner, and P. Carretta, *Phys. Rev. B* **94**, 054508 (2016).
- [35] R. M. Fernandes and A. J. Millis, *Phys. Rev. Lett.* **110**, 117004 (2013).
- [36] G. S. Tucker, D. K. Pratt, M. G. Kim, S. Ran, A. Thaler, G. E. Granroth, K. Marty, W. Tian, J. L. Zarestky, M. D. Lumsden, S. L. Bud'ko, P. C. Canfield, A. Kreyssig, A. I. Goldman, and R. J. McQueeney, *Phys. Rev. B* **86**, 020503(R) (2012).
- [37] M. N. Gastiasoro and B. M. Andersen, *Phys. Rev. B* **92**, 140506(R) (2015).
- [38] See Supplemental Material at <http://link.aps.org/supplemental/10.1103/PhysRevB.95.180501> for details about the composition of the samples, the Mössbauer measurements, NQR and NMR spectra, and the theoretical methods used in Rapid Communication.
- [39] H.-H. Klauss, H. Luetkens, R. Klingeler, C. Hess, F. J. Litterst, M. Kraken, M. M. Korshunov, I. Eremin, S.-L. Drechsler, R. Khasanov, A. Amato, J. Hamann-Borrero, N. Leps, A. Kondrat, G. Behr, J. Werner, and B. Büchner, *Phys. Rev. Lett.* **101**, 077005 (2008).
- [40] S. Kitao, Y. Kobayashi, S. Higashitaniguchi, M. Saito, Y. Kamihara, M. Hirano, T. Mitsui, H. Hosono, and M. Seto, *J. Phys. Soc. Jpn.* **77**, 103706 (2008).
- [41] M. A. McGuire, A. D. Christianson, A. S. Sefat, B. C. Sales, M. D. Lumsden, R. Jin, E. A. Payzant, D. Mandrus, Y. Luan, V. Keppens, V. Varadarajan, J. W. Brill, R. P. Hermann, M. T. Sougrati, F. Grandjean, and G. J. Long, *Phys. Rev. B* **78**, 094517 (2008).
- [42] K. Kitagawa, N. Katayama, K. Ohgushi, M. Yoshida, and M. Takigawa, *J. Phys. Soc. Jpn.* **77**, 114709 (2008).
- [43] S. Kitagawa, Y. Nakai, T. Iye, K. Ishida, Y. Kamihara, M. Hirano, and H. Hosono, *Phys. Rev. B* **81**, 212502 (2010).
- [44] P. C. Riedi, *Hyperfine Interact.* **49**, 335 (1989).
- [45] M. Fu, D. A. Torchetti, T. Imai, F. L. Ning, J.-Q. Yan, and A. S. Sefat, *Phys. Rev. Lett.* **109**, 247001 (2012).
- [46] G. Lang, L. Veyrat, U. Gräfe, F. Hammerath, D. Paar, G. Behr, S. Wurmehl, and H.-J. Grafe, *Phys. Rev. B* **94**, 014514 (2016).
- [47] G. Lang, H.-J. Grafe, D. Paar, F. Hammerath, K. Manthey, G. Behr, J. Werner, and B. Büchner, *Phys. Rev. Lett.* **104**, 097001 (2010).

- [48] Y. Kobayashi, E. Satomi, S. C. Lee, and M. Sato, *J. Phys. Soc. Jpn.* **79**, 093709 (2010).
- [49] D. Bérardan, L. Pinsard-Gaudart, and N. Dragoe, *J. Alloys Compd.* **481**, 470 (2009).
- [50] H. Ikeda, R. Arita, and J. Kunes, *Phys. Rev. B* **81**, 054502 (2010).
- [51] B. M. Andersen, P. J. Hirschfeld, A. P. Kampf, and M. Schmid, *Phys. Rev. Lett.* **99**, 147002 (2007).
- [52] M. N. Gastiasoro and B. M. Andersen, *Phys. Rev. Lett.* **113**, 067002 (2014).
- [53] S. Doniach, *Physica B+C* **91**, 231 (1977).
- [54] Z. F. Weng, M. Smidman, L. Jiao, Xin Lu, and H. Q. Yuan, *Rep. Prog. Phys.* **79**, 094503 (2016).
- [55] L. D. Pham, Tuson Park, S. Maquilon, J. D. Thompson, and Z. Fisk, *Phys. Rev. Lett.* **97**, 056404 (2006).
- [56] Y. P. Wu, D. Zhao, A. F. Wang, N. Z. Wang, Z. J. Xiang, X. G. Luo, T. Wu, and X. H. Chen, *Phys. Rev. Lett.* **116**, 147001 (2016).
- [57] K. Haule and G. Kotliar, *New J. Phys.* **11**, 025021 (2009).